Abdulaleem N. Abed
Wallaa M. Mohammad

Department of Physics,
College of Education for
Pure Sciences,
University of Tikrit,
Tikrit, IRAQ

Structural and Optical Characteristics of CNTs-Doped ZnO Thin Films Prepared by Spray Pyrolysis

This study examines the structural and optical characteristics of zinc oxide (ZnO) thin films infused with 0.05 wt.% carbon nanotubes (CNTs), produced using thermal spray pyrolysis at 400±2°C. X-ray diffraction (XRD) verified a polycrystalline structure with a predominant (101) orientation. Atomic force microscopy (AFM) demonstrated an approximate 10% decrease in root mean square surface roughness attributable to the introduction of CNTs, signifying improved surface uniformity and crystallinity. Optical studies indicated alterations in absorbance and transmittance, as well as an expansion of the optical band gap from 3.85 to 3.95 eV. The results indicate enhanced electronic transport and lattice ordering, reinforcing the promise of CNTs-doped ZnO thin films for future optoelectronic and photonic applications.

Keywords: Zinc oxide; Carbon nanotubes; Spray pyrolysis; Optical properties
Received: 22 April 2025; **Revised:** 12 June 2025; **Accepted:** 19 June 2025

1. Introduction

Zinc oxide (ZnO) is a potential photoelectrical nanomaterial for photocatalysis and the destruction of diverse organic contaminants, due to its high sensitivity, exceptional stability, broad bandgap, and eco-friendliness [1,2]. ZnO is a crucial functional metal oxide due to its many uses, including the production of photodetectors, transparent electrodes, spintronic devices, surface acoustic wave devices, and thin-film gas sensors. The versatility of ZnO stems from its exceptional characteristics, which include a broad direct optical bandgap, considerable exciton binding energy, and excellent chemical and thermal stability, in addition to its piezoelectric features [3,4].

Nanomaterials with distinctive characteristics, including quantum effects and optical properties, are appropriate for biological applications. Carbon nanotubes (CNTs) have considerable potential uses that leverage their distinctive characteristics [3-6]. Multi-walled carbon nanotubes (MWCNTs) are extensively used as supports for heterogeneous catalysts because to their substantial surface area, remarkable mechanical strength, and stability under extreme environments. CNTs consist of layers of carbon atoms organized in hexagonal patterns. They have unique geometries characterized by an amorphous configuration of aromatic layers with varying molecular dimensions that create porosity. CNTs consist of bent sp^2-hybridized carbon atoms organized in an axial configuration of concentric cylindrical layers [7]. An interesting use of nanoparticles, namely CuO doped with ($ZnO_{1-x}CNTs_x$), is the development of biosensors for *in vivo* usage, due to the low toxicity of these carbon-based materials. CNTs are attracting significant interest because to their distinctive fundamental physical structures and exceptional mechanical and electrical capabilities, which facilitate prospective high-technology applications [8].

Recently, nanostructured materials, including ZnO/CuO:CNTs composites, have been used in electrochemical sensors for biological and pharmacological investigations. They have several features similar to other materials, however provide distinct advantages such as improved electron transport, elevated edge plane/basal plane ratios, and accelerated kinetics of electrode operations [9].

The aim of this study is to evaluate how doping ZnO with CNTs influences its structural and optical characteristics when synthesized via spray pyrolysis. This research is motivated by the potential of ZnO-CNTs nanocomposites to improve light absorption, carrier transport, and surface morphology, making them promising materials for applications in sensors, optoelectronics, and solar cells.

2. Experimental Part

The cleaning procedure is a crucial aspect for success in acquiring deposited membranes devoid of undesirable contaminants. Glass slides with dimensions of 2.5x2.5 cm^2 were sued. They were cleaned after washed thoroughly with distilled water at a temperature of 80°C to remove airborne contaminants. Then, they were washed again with distilled water at 80°C and immersed in ethanol. After that, they were immersed in methanol solution to remove any oily residues or contaminants. They were dried using a hair dryer. Samples of $ZnO_{1-x}CNTs_x$ were weighed with weight ratios (x=0 and 0.05 wt.%), as ZnO and CNTs were supplied by Sigma-Aldrich Chemie GmbH. They were mixed using a mortar made of agate and placed in a beaker. 200 mL of

deionized (DI) water was added at a temperature of 37°C. The mixture was treated with an ultrasonic device for 3 hours to prevent agglomeration of the mixed materials. It was then placed on a magnetic stirrer for 3 hours at a temperature of 37°C. The solution was then sprayed using a thermal spray device on the glass substrates after adjusting the spray device to a temperature of 400±2 °C with 10 sprays for a spray time of 3 s, and a stop time of 10 s. Then the optical characterization was carried out on the samples. Figure (1) and tables (1) and (2) illustrate the steps followed in sample preparation, the weight ratios of each material and operating parameters of the thermal spray pyrolysis system, respectively.

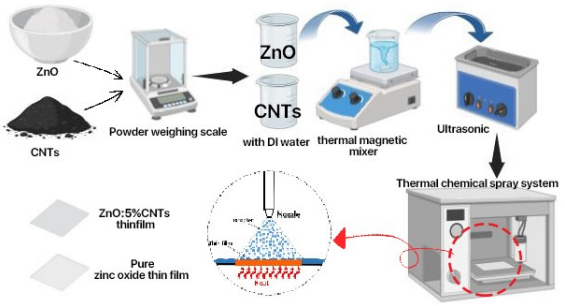

Fig. (1) Schematic illustration of the sample preparation steps for ZnO and CNTs-doped ZnO thin films

Table (1) Molar ratios of starting materials used for ZnO and CNTs-doped ZnO thin films

X	$ZnO_{1-x}CNTs_x$
0	ZnO
0.05	$ZnO_{0.95}CNTs_{0.05}$

Table (2) Operating parameters of the thermal spray pyrolysis system

Terms of Operation	
400±2°C	Temperature
4 bar	Pressure
30±0.5cm	The distance between the nozzle and the base
$(10s)_{off}$ $(3s)_{on}$	Spraying time and stopping time
10 sprays	Number of sprays
10 mL/min	Spray rate

3. Results and Discussion

The XRD pattern of the undoped ZnO thin film (x=0) exhibits a polycrystalline hexagonal structure with multiple diffraction peaks, predominantly at 2θ = 36.27°, corresponding to the (101) plane, as shown in Fig. (2) and table (3). These peaks matched the standard JCPDS card no. 00-036-1451. When CNTs were incorporated at 0.05 wt.%, the number of peaks decreased to only three, and their intensity significantly dropped, particularly for the dominant (101) plane, now appearing at 2θ = 36.68°, as shown in Fig. (2). This reduction in peak number and intensity indicates increased lattice disorder and structural distortion, likely due to strain introduced by the CNTs network. The peak shift and crystallite size variation suggest changes in the growth dynamics and crystal orientation upon doping, in agreement with [10,11].

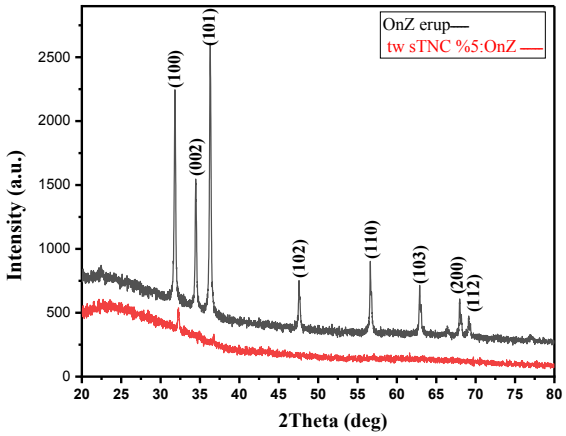

Fig. (2) XRD patterns of pure and CNTs-doped ZnO thin film (x=0 and 0.05 wt.%), showing reduced peak intensity and number

AFM analysis, presented in figures (3) and (4) and table (4), show a decrease in surface roughness upon doping. The RMS value for the undoped film (x=0) was 3.30410 nm, while for the CNTs-doped film (x=0.05 wt.%), it was 3.03142 nm. This reduction (~8.3%) reflects enhanced film uniformity and reduced grain boundary roughness. The histogram profiles showed a shift in peak height distribution from 240-400 nm (x=0) to 160-240 nm (x=0.05), with a higher percentage of surface regions at lower height values. This suggests that CNTs served as nucleation centers, influencing the crystal growth mechanism and leading to finer grain structures, which is consistent with [12].

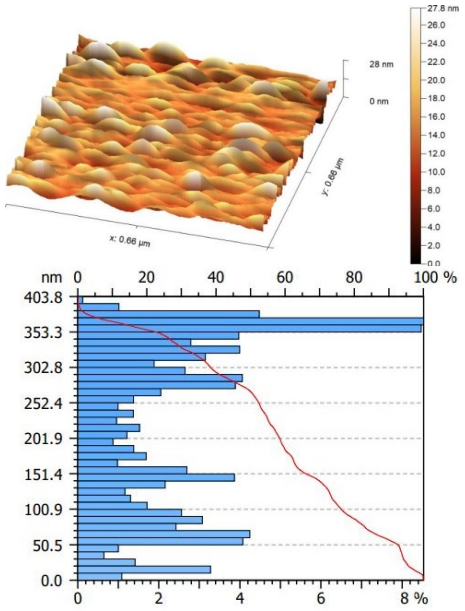

Fig. (3) AFM results of pure (undoped) ZnO thin film (x=0)

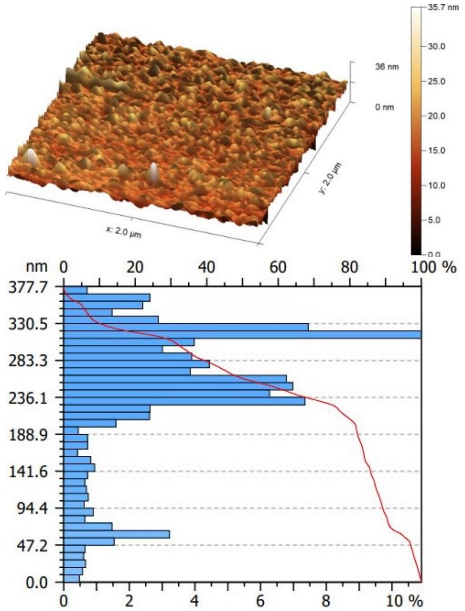

Fig. (4) AFM results of (ZnO_{1-x} $CNTs_x$) (x=0.05)

The optical absorption spectra in Fig. (5) show high absorbance in the UV-visible region for both samples, with stronger absorption in the undoped film. Upon doping with CNTs (x=0.05 wt.%), a slight decrease in absorbance was observed, suggesting improved crystallinity and reduced optical scattering due to lower defect density. The transmission spectra in Fig. (6) show an opposite trend, where the doped film exhibited higher transmittance (up to ~35%) in the spectral range 400-1100 nm, compared to the undoped film (~5%), especially at wavelengths longer than 300 nm. This improvement supports the potential of CNTs-doped ZnO films in transparent electronics and sensors [13,14].

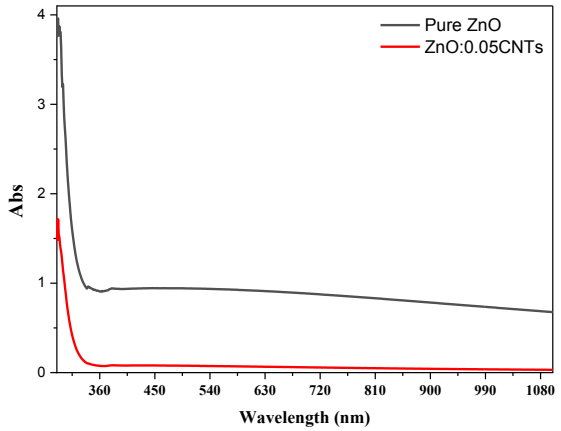

Fig. (5) UV–visible absorption spectra of ZnO and CNTs-doped ZnO thin films

The absorption coefficient (α), shown in Fig. (7), displays a typical increase with photon energy, exceeding 10^4 cm^{-1}, indicating a direct bandgap transition. The undoped film exhibited an optical band gap (E_g) of 3.85 eV, while the doped film's bandgap widened slightly to 3.95 eV, as calculated from Tauc's plots in Fig. (8). This shift suggests an upward Fermi level movement, possibly due to enhanced carrier concentration or quantum confinement effects induced by CNTs doping [15,16].

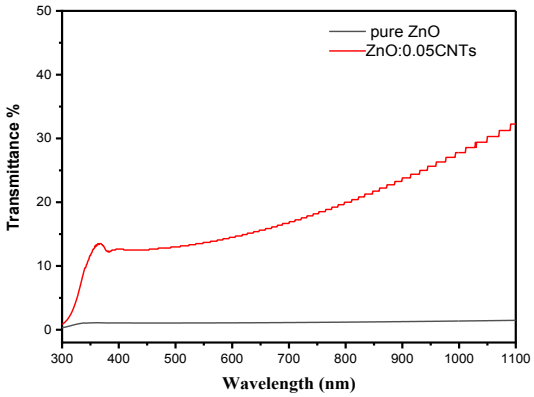

Fig. (6) Optical transmission spectra of ZnO and CNTs-doped ZnO thin films

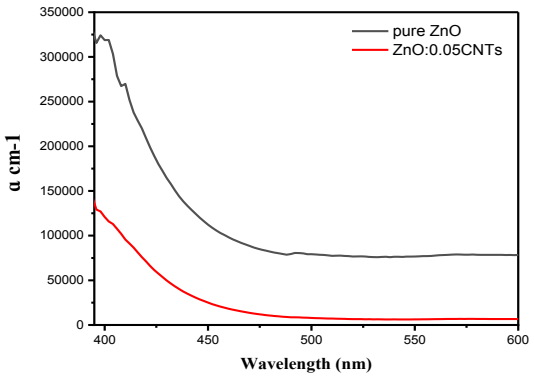

Fig. (7) Absorption coefficient as a function of photon energy for both pure (undoped) and doped ZnO thin films

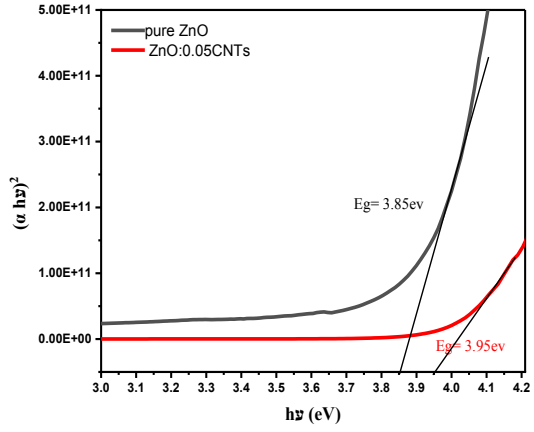

Fig. (8) The calculated optical bandgap for the prepared films

As shown in Fig. (9), the extinction coefficient (k) decreased with increasing wavelength, particularly in the visible region, consistent with lower absorption in the doped film. At 400 nm, a rise in k is observed in the undoped sample, while in the doped film, k remains lower due to reduced reabsorption. Figure

(10) presents the reflection spectra, where the undoped film showed minimal reflectance, while the CNTs-doped film exhibited higher reflectivity. This is attributed to the darker appearance of the film after CNTs addition, which increased its opacity. These optical changes confirm the strong influence of CNTs on the ZnO thin film's optical behavior [15,16].

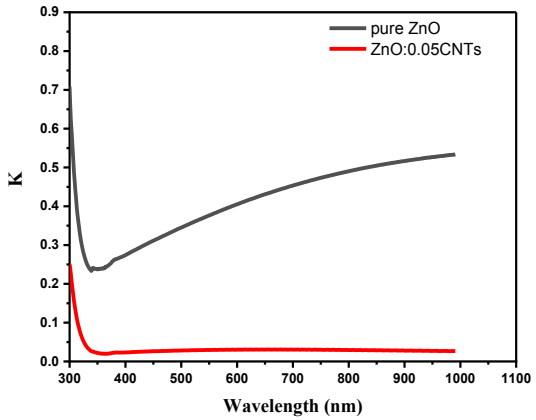

Fig. (9) Extinction coefficient (k) versus wavelength for ZnO and CNTs-doped ZnO thin films

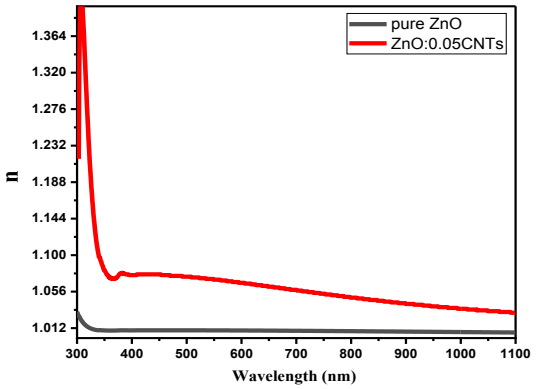

Fig. (10) Reflection spectra of ZnO and CNTs-doped ZnO thin films

4. Conclusion

In this study, ZnO thin films doped with 0.05 wt.% CNTs were successfully synthesized using the spray pyrolysis technique. The incorporation of CNTs led to a reduction in surface roughness and improved crystallinity. Optically, the doped films exhibited enhanced transmittance and reflectance, along with a slight increase in the optical band gap from 3.85 to 3.95 eV. These improvements indicate reduced structural defects, better electronic transitions, and enhanced surface uniformity. Such enhancements make CNTs-doped ZnO thin films promising candidates for optoelectronic applications, including sensors and solar energy devices.

References

[1] J. Smith and A. Johnson, "Synthesis and characterization of ZnO thin films by spray pyrolysis", *J. Mater. Sci.*, 45 (2020) 123–130.

[2] A.R. Bbagheri and S. Ibrahimi, "Enhancement of Photoluminescence Characteristics of Zinc Oxide Nanostructures Using Inclined Pulsed Laser Irradiation", *Iraqi J. Appl. Phys. Lett.,* 8(1) (2025) 17-20.

[3] A. Hussain and Q.N. Abdullah, "Characterization of ZnO-SnO_2 Nanostructures Prepared by Thermal Evaporation Technique as Gas Sensor", *Iraqi J. Appl. Phys.*, 19(4C) (2023) 243-250.

[4] A.A. Hameed and M.M. Khalaf, "Extraction of Zinc oxide Nanopowders Prepared by Physical Vapor Deposition Technique", *Iraqi J. Appl. Phys. Lett.,* 7(1) (2024) 3-6.

[5] K. Nguyen and M. Tran, "AFM analysis of ZnO thin films", *Surf. Interface Anal.*, 52(5) (2020) 234–240.

[6] P. Singh, "Band gap engineering in ZnO nanostructures", *Semicond. Sci. Technol.*, 35(4) (2020) 045001.

[7] S. Wang and V. Zhao, "Reflectance studies of CNTs ZnO films", *J. Appl. Phys.*, 127(12) (2020) 125301.

[8] R. Verma, "Optical band gap modification in ZnO films", *J. Phys. D: Appl. Phys.*, 53(15) (2020) 155101.

[9] H.S. Lokesha et al., "Impact of Cr doping on the structure, optical and magnetic properties of nanocrystalline ZnO particles", *J. Alloys Comp.*, 960 (2023) 170815.

[10] F.Z. Bedia et al., "Effect of tin doping on optical properties of nanostructured ZnO thin films grown by spray pyrolysis technique", *J. Alloys Comp.,* 616 (2014) 312-318.

[11] A. Smith, "Spray pyrolyzed surface-modified ZnO thin films via cobalt doping", *Appl. Surf. Sci.*, 589 (2022) 152942.

[12] E.F. Johnson, "Carbon nanotube doping effects on ZnO films", *Nanotech.*, 31(7) (2020) 075701.

[13] M. Irfan et al., "Testing of Sr-doped ZnO/CNT photocatalysts for hydrogen evolution from water splitting under atmospheric dielectric barrier plasma exposure", *ACS Omega*, 5 (2023) 18891-18900.

[14] G.H. Lee and I.J. Kim, "Optical properties of CNTS doped ZnO", *Opt. Mater.*, 98 (2020) 109482.

[15] H.I.J. Kwon, "Crystallographic orientation in ZnO films", *Cryst. Eng. Commun.*, 22(10) (2020) 1800-1806.

[16] A.H. Mansoor and W.M. Mohammd, "Effect of Doping with Carbon Nanotubes on Structural and Optical Properties of Nanostructured Zinc Oxide Thin Films", *Iraqi J. Appl. Phys.,* 20(4) (2024) 793-796.

Table (3) XRD data for ZnO and CNTs-doped ZnO thin films

Sample ($ZnO_{1-x}CNTs_x$)	Position [2θ] (deg)	Intensity (counts)	FWHM Left (deg)	d-spacing (Å)	C.S. (nm)	(hkl)	Structure	JCPDS card
x=0	31.7934	1258.09	0.1788	2.81230	50.28478	100	Hexagonal	36-1451
	34.4495	816.50	0.1543	2.60130	58.67211	002	Hexagonal	
	36.2777	1621.90	0.1762	2.47429	51.64171	101	Hexagonal	
	47.5727	278.69	0.1564	1.90986	60.42061	102	Hexagonal	
	56.5392	31.03	0.6985	1.62640	14.05597	110	Hexagonal	
	56.6325	456.58	0.1302	1.62395	75.44085	110	Hexagonal	
	62.8913	302.70	0.1953	1.47655	51.89783	103	Hexagonal	
	66.3202	37.57	2.3451	1.40827	4.40460	200	Hexagonal	
	67.9805	286.19	0.1350	1.37787	77.25233	112	Hexagonal	
	69.1442	50.63	1.1891	1.35749	8.83148	201	Hexagonal	
x=0.05	32.1645	87.67	1.1440	2.78069	7.86649	100	Hexagonal	00-036-1451
	36.6839	10.98	0.0370	2.44782	246.21360	101	Hexagonal	

Table (4) AFM-based surface roughness parameters of ZnO and CNTs-doped ZnO films

Sample ($ZnO_{1-x}CNTs_x$)	Skewness (Ssk)	Density (particles/mm^2)	RMS (nm)	Surface Thickness (nm)	Roughness Average (nm)	Root Mean Square (nm)
x =0	0.169005	750000	3.30410	49.5	1.670	1.97
x=0.05	0.037020	2000000	3.03142	36.0	2.380	2.16

